A&A 466, 1185–1188 (2007)
DOI: 10.1051/0004-6361:20066866


Astronomy & Astrophysics

# Properties of the icy surface of the TNO 136108 (2003 $EL_{61}$)⋆

F. Merlin[1], A. Guilbert[1], C. Dumas[2], M. A. Barucci[1], C. de Bergh[1], and P. Vernazza[1]

[1] LESIA, Observatoire de Paris, 92195 Meudon Principal Cedex, France
e-mail: frederic.merlin@obspm.fr
[2] ESO, Alonso de Cordova 3107, Vitacura Casilla 19001 Santiago 19, Chile
e-mail: cdumas@eso.org

Received 4 December 2006 / Accepted 6 February 2007

**ABSTRACT**

*Context.* Spectroscopic observations of numerous trans-Neptunian objects (TNOs), considered to be among the most pristine objects of the solar system, have revealed the presence of several kinds of surface ices. The high-sensitivity spectra that can be measured for the brightest objects also provide constraints on the physical properties of the surface (e.g. ice phase, temperature).
*Aims.* We observed one of the largest and brightest TNOs, 136108 (2003 $EL_{61}$), to determine its surface composition properties and to constrain its surface properties.
*Methods.* We obtained new visible spectra with EMMI on the ESO-NTT and near-infrared spectra with the new 3D spectrograph SINFONI at the ESO-VLT. Our analysis consists of radiative transfer modelling to constrain composition and surface properties and to identify the precise minimum of the 1.65 micron band to constrain the surface temperature.
*Results.* The observations reveal a surface essentially composed of water ice. An absorption feature at 1.65 micron clearly indicates the presence of ice in the crystalline phase. Spectral modelling suggests that a small fraction of the surface ice is in the amorphous state. We also derive the temperature of the crystalline ice at the surface.

**Key words.** Kuiper Belt – radiative transfer

## 1. Introduction

Recent discoveries of numerous objects orbiting the Sun beyond Neptune have opened a new window onto the origin and evolution of our Solar System. These trans-Neptunian objects (TNOs) are supposed to be the most primitive Solar System bodies and deep investigation of them (dynamical studies, photometric and spectroscopic observations) can give rich insights into the formation and evolution of protoplanetary disks and extrasolar planetary systems. In this paper we report on new observations of TNO 136108 (2003 $EL_{61}$) carried out at ESO-VLT in the near infrared with the new 3D spectrograph SINFONI in $H$ and $K$ bands, as well as visible spectroscopy carried out at ESO-NTT with the spectrograph EMMI in the 0.5–0.9 $\mu$m range. The object 2003 $EL_{61}$ is one of the largest known TNOs. It is in a classical orbit with high inclination (28°).

Rabinowitz et al. (2005) observed it by photometry, obtaining a rotational period of 3.9154 ± 0.0002 h and a large amplitude of 0.28 mag, which defines 2003 $EL_{61}$ as the most rapid large rotator in the Solar System with an elongated shape. Two satellites with circular orbits have been discovered (Brown et al. 2005, 2006). Observations of the orbit of the first detected satellite (Brown et al. 2005) have allowed the mass of the system (32% of the Pluto mass) to be estimated, and with this estimation, Rabinowitz et al. (2006) gave constraints on the size and albedo of 2003 $EL_{61}$: a total length of 1960–2500 km and a visual albedo greater than 0.6. They also derived a mean density of 2600–3300 kg m$^{-3}$, suggesting that it has lost most of its volatiles.

Tegler et al. (2006) observed this body with visible spectroscopy (with 20 Å resolution) at the 6.5 m MMT telescope on Mt Hopkins, obtaining a featureless spectrum with a possible band at 5773 Å associated to $O_2$-ice. Trujillo et al. (2007), using Gemini and Keck telescopes, detected a surface covered by pure crystalline water ice with a near infrared spectrum very similar to that of Charon. They found a best-fitted model with pure crystalline water ice combined with blue material, such as hydrogen cyanide ice or possible phyllosilicate clays, suggesting some kind of global surface renewal process. Barkume et al. (2006) also reported their observations of its brightest satellite (S/2005 $EL_{61}$) observed simultaneously. They detected deep water ice features, but the poor resolution of the spectrum of the faint satellite does not allow derivation of the ice phase (crystalline or amorphous). Brown et al. (2007) suggested that 2003 $EL_{61}$ has experienced a giant impact that created its satellite system. In fact, through the results of their survey carried out at the Keck telecope on bright TNOs, Brown et al. (2007) have discovered a subclass of objects with spectral and orbital properties similar to those of 2003 $EL_{61}$.

Our $H + K$ observations of 2003 $EL_{61}$ have been combined with our new visible observations. The analysis of the combined spectra (visible and near-infrared) is presented, together with radiative transfer models used to investigate the surface composition, and we compare our results with those of Trujillo et al. (2007). Finally we discuss the possibility of obtaining constraints on the surface temperature of this object.

⋆ Based on observations obtained at the VLT Observatory, Cerro Paranal of European Southern Observatory, ESO, Chile, in the framework of program 275.C-5048D

## 2. Observations and data reductions

The TNO 2003 $EL_{61}$ was observed with the ESO-VLT (Very Large Telescope), for the near infrared spectroscopy, and with the ESO-NTT (New Technology Telescope) for the visible part of the spectra.

### 2.1. Near infrared spectroscopy

Near infrared spectra were obtained with SINFONI (Spectrograph for INtegral Field Observations in the Near Infrared), an integral field spectrometer installed at the VLT. More information about this instrument can be found in a paper describing observations of the large TNO Eris (Dumas et al. 2007). 2003 $EL_{61}$ has been observed on February 25, 2006 at 8:20 UT (airmass ranging from 1.400 to 1.437) and on March 12, 2006 at 6:00 UT (airmass ranging from 1.425 to 1.481) with the no-AO mode and the $H + K$ grating. This mode covers the $H$ and $K$ bands at the same time, with a spectral resolution of 1500. The Xe-Ar-Kr lamps provide the wavelength calibration with an accuracy of 0.0005 $\mu$m per pixel. Each night, several cubes of data (with an individual exposure time of 600 s) were taken (4 the first night, 3 the second one) and a solar analog, BD+192729, was observed at similar airmasses (1.387 in February and 1.427 in March), with the same instrumental setting providing the needed calibrations.

The data were reduced mainly using the Max Planck Institute data reduction package that provides the bad pixel correction, the sky substraction, and the flat field division. The wavelength calibration has obtained with the ESO SINFONI pipeline. For each night, the individual cubes were co-added in order to improve the signal-to-noise ratio. The spectra were extracted from the resulting cube using QFitsView, a visualization tool developed by the Max Planck Institute. They were finally divided by the solar analog spectrum in order to remove the solar and telluric features. The division of the object spectra by good analog spectra allows the real spectral reflectance of our object to be obtained along the wavelength range.

### 2.2. Visible spectroscopy

The visible spectrum was taken on February 01, 2006 at the NTT, using EMMI (ESO Multi-Mode Instrument) at 8:08 UT (airmass 1.6) with an exposure time of 900 s. We observed the solar analog star Landolt 102-1081 at a similar airmass to obtain the calibration data. Standard techniques for the visible spectroscopy was applied. An average bias was created and subtracted for the spectrum, which is then divided by a normalized flat field, and calibrated in wavelength. The resulting spectrum is finally divided by the solar analog spectrum in order to remove the solar response and the telluric absorption features.

## 3. Results and surface modelling

Figures 1 and 2 show the two near-infrared spectra (February and March, respectively) adjusted with the visible spectrum obtained in February. We used the object's color determined by Trujillo et al. (2007): $V - H = 1.007$ and the solar indice $V - H = 1.37$ from Hartmann et al. (1982) to compute the relative reflectance in the $H$ band. We used a mean albedo of 0.65 in the $V$ band, according to the results of Barkume et al. (2006) who give albedo values between 0.6 and 0.72 (due to the several possible shapes of the body). Due to the poor signal-to-noise level of our visible spectrum, we were not able to detect the absorption band near 0.5773 $\mu$m observed by Tegler et al. (2006). We confirm clear evidence of a crystalline water ice band near 1.65 $\mu$m in both spectra. We also detected the 1.5 and 2.0 $\mu$m bands, which are attributed to either crystalline or amorphous water ice. Due to the relatively high airmass during the observations and some airmasses' difference with the analog star, the telluric bands are not totally removed. We therefore restricted our analysis to the 1.5–1.75 $\mu$m and 1.95–2.3 $\mu$m parts of the spectrum, which are less affected by this problem. To investigate the surface properties of this object better, we ran a radiative transfer model, based on the Hapke theory (1981 and 1993). We used the optical constants of amorphous water ice at 38 K (Schmitt et al. 1998), crystalline water ice from 20 to 80 K (Grundy & Schmitt 1998), and amorphous carbon (Zubko et al. 1996). We used the method described in Barucci et al. (2006) to obtain the models.

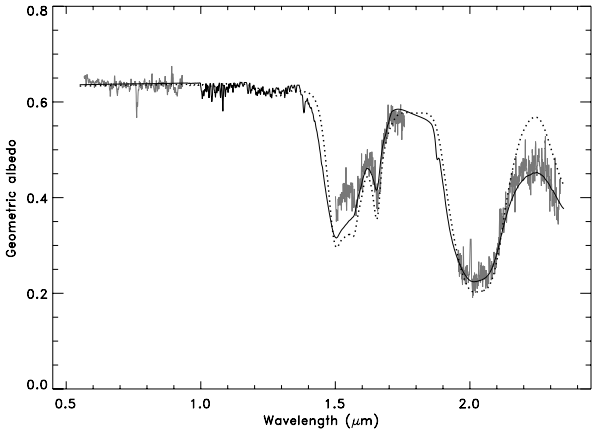


**Fig. 1.** Spectrum of 2003 $EL_{61}$ obtained on February 01, 2006 (visible part) and February 25, 2006 (nIR part). The intimate models computed with Hapke theory in continuous and dotted lines are overlapped. The model plotted in a continuous line corresponds to an intimate mixture of 87% crystalline water ice (particle size of 10 $\mu$m), 10% amorphous water ice (150 $\mu$m), and 3% amorphous carbon (15 $\mu$m). The dotted line corresponds to an intimate mixture of 97% crystalline water ice (particle size of 20 $\mu$m) and 3% amorphous carbon (15 $\mu$m). The agreement of this second mixture is worse in the nIR, especially in the $K$ band where the model requires a bluish component.

The best fits of our model indicate the presence of large amounts of amorphous and crystalline water ice (see Figs. 1 and 2), and a small amount of amorphous carbon. The particle sizes were limited to the 10–450 $\mu$m range. If the upper limit was arbitrary, the lower was defined according to the limit of the model that requires a larger particle size than the wavelength. The carbon component does not show any absorption feature in our wavelength range; it is introduced into the model to reproduce the albedo of the object. We also note that the size dependence of the carbon albedo is negligible and that the size of carbon particles cannot be constrained. The differences between the spectra from the two nights (Figs. 1 and 2) are minor. Each spectrum, acquired in 30 or 40 min, is an average spectrum of 57 or 66% of the object's surface, according to the rotation period determined by Rabinowitz et al. (2006), and the difference in rotational phase is about 70%. Only 30% of the surface observed during the first run was observed during the second run. It therefore seems that 2003 $EL_{61}$ is homogeneous even if a better signal-to-noise level is needed to compare the water ice bands.

A simple mixture of crystalline water ice and amorphous carbon fits the spectrum quite well but does not allow fit of the $K$ band behavior (see Fig. 1). Amorphous water ice, mixed

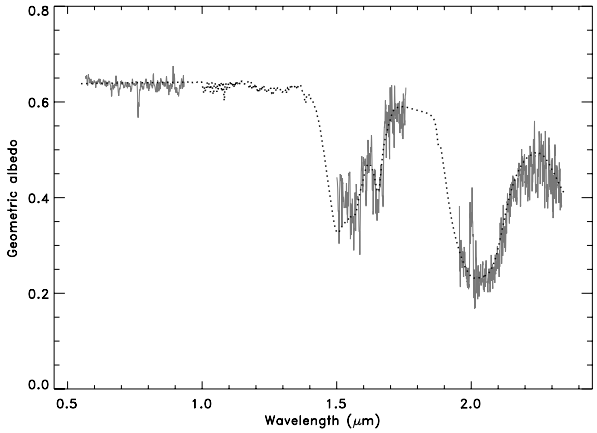


**Fig. 2.** Spectrum of 2003 $EL_{61}$ obtained on February 01, 2006 (visible part) and March 12, 2006 (nIR part) and the intimate model computed with the Hapke theory with a dotted line. This model correspond to an intimate mixture of 88% crystalline water ice (particle size of 10 $\mu$m), 9% amorphous water ice (130 $\mu$m), and 3% amorphous carbon.

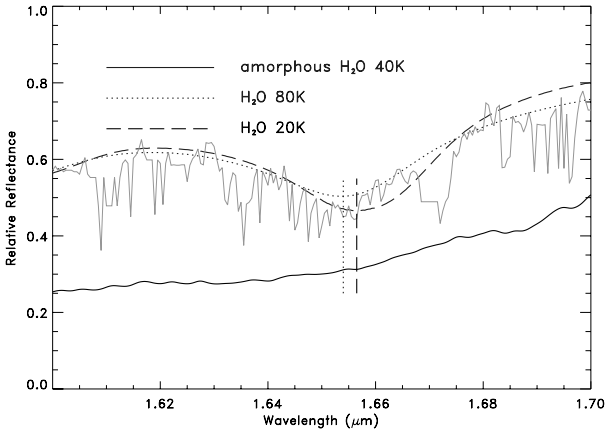


**Fig. 3.** Spectral reflectance of the object (grey continuous line), of pure amorphous water ice (black line), and of pure crystalline water ice at 20 and 80 K (respectively with a dashed line and dotted line) around 1.65 $\mu$m. The reflectance of the icy components are given for a particle size of 10 $\mu$m (crystalline) and 150 $\mu$m (amorphous). The vertical lines (dotted or dashed) give the position of the minimum of the absorption band.

with crystalline water ice, has been observed on several Galilean satellites by Hansen & McCord (2004). The use of amorphous water ice in our models improves the fit over the entire 0.5–2.4 $\mu$m range considerably. Amorphous water ice is bluer than crytalline water ice in the near infrared, its absorption bands are shifted compared to those of crystalline water ice, and the mixture of the two phases generates larger absorption bands (especially for the 2.0 $\mu$m band). The best fits on both spectra give similar results with large amounts of crystalline water ice, close to 90%. Our models are non-unique, but represent the best fit for the visible and near-infrared range, even if it is not optimized around 1.5 $\mu$m. Similar results have been also found by other authors. In fact, this mixture of water ice in both states has also been used to reproduce the spectra of Uranian satellites with an upper limit of 10–20% of amorphous water ice (Grundy et al. 2006). Our results also agree with the Brown et al. (2007) suggestion, who offer the hypothesis that 2003 $EL_{61}$ has experienced a giant impact. Crystalline water ice could be produced by heating from the shock. Then, a part of the ice has been amorphized by irradiation (see below). However, Trujillo et al. (2007) do not report any improvement using amorphous water ice, probably due to the fact that the combination of particle sizes of crystalline and amorphous water ice is different from ours. Trujillo et al. (2007) instead use several other blue components in the near infrared to improve the fit, like hydrogen cyanide, hydrated Tholins, or phyllosilicate clays, which show that other possible materials could fit this TNO's spectrum.

The use of amorphous water ice to reproduce the spectra of cold objects is physically consistent. Indeed, laboratory experiments on ice deposition indicate that, at the low temperatures characteristic of TNOs, water ice should be amorphous. Furthermore, TNOs are subjected to various space weathering processes; among them, irradiation by high-energy charged particles should rapidly transform crystalline ice, if present on the surface, into amorphous ice (e.g. Strazzulla et al. 1991; Mastrapa & Brown 2002). Laboratory experiments show that this mechanism is particularly efficient below 70 K (e.g. Moore & Hudson 1992; Mastrapa & Brown 2006). In contrast, it is difficult to explain the predominance of crystalline ice on TNOs (as well as on Charon and all icy outer planet satellites). Either the amorphization mechanisms (bulk and/or surfacial) are not as efficient as expected or other mechanisms predominate. Jewitt & Luu (2004) have considered several mechanisms: internal heating and subsequent cryovolcanism as a possible crystallization process or impact heating by micrometeorites that could heat surface ice above the crystallization temperature. Grundy et al. (2006) suggest that, for a body with an amorphous bulk composition, non-thermal energy inputs from less energetic charged particles could efficiently transform amorphous ice to crystalline ice, at least down to the depths probed by near-infrared spectroscopy (mm depths). The presence of both the amorphous and crystalline phases of water in the uppermost surface layers of 2003 $EL_{61}$ would not be too surprising.

## 4. Ice temperature determination

According to Barkume et al. (2006), who determined an albedo between 0.6–0.7, we can assume a mean surface temperature of about 30 K using the Stefan-Boltzmann law. From laboratory experiments, it is possible to link the absorption behavior of crystalline water ice with the temperature of the ice. Usually, the depth and the width of the 1.65 $\mu$m band are the main indicators: the width and depth of this band both increase with decreasing deposition temperature. However, in our model, particle size and amount of crystalline water ice on the surface of the objects modify the behavior of this absorption band, and it is not possible to use the depth and width values to obtain the surface temperature.

Fink & Larson (1975) described a method of accessing the temperature of a body. The method requires computing the ratio between the 1.65 $\mu$m band area and the entire 1.5 $\mu$m band absorption area. This method cannot be used in our case where the data in the near infrared range begin at 1.5 $\mu$m, whereas the large 1.5 $\mu$m band begins at about 1.4 $\mu$m. Moreover, the 1.65 $\mu$m band is more or less destroyed after irradiation, which affects the surface of TNOs (e.g. Mastrapa & Brown 2006), and therefore the temperature determination using the depth of the 1.65 $\mu$m may not be appropriate.

One of the most striking changes in the behavior of the crystalline water ice spectrum with temperature is the wavelength shift (Grundy & Schmitt 1998). Thus, this ice could be used as a spectral thermometer. In Fig. 3, we report several reflectance

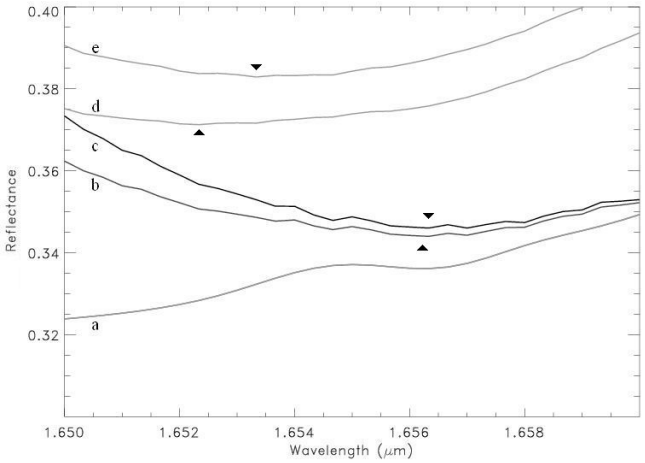


**Fig. 4.** Reflectance of amorphous water ice (*a*), of crystalline water ice (*c* at 20 K and *e* at 80 K), and of mixtures of amorphous and crystalline water ice (*b* and *d* with, respectively, amorphous water ice at 38 K with crystalline water ice at 20 or 80 K with the ratio 0.25:0.75). Each black triangle indicates the minimum of the 1.65 $\mu$m absorption band.

spectra between 1.55 and 1.75 $\mu$m: the object spectrum taken in February (its noise is less than in March), the reflectance spectrum of amorphous water ice at 38 K, and reflectance spectra of crystalline water ice at 20 K (central wavelength of the band at 1.656 $\mu$m) and 80 K (central wavelength of the band at 1.653 $\mu$m). Figure 3 shows laboratory results where the central wavelength measurement determines the temperature of the crystalline water ice. However, potential effects can shift the apparent wavelengths or shapes of the water ice bands in the spectra of planetary surfaces (Grundy et al. 1999). In our case, crystalline water ice is mixed with amorphous water ice and amorphous carbon (completely featureless in terms of reflectance in the near infrared range), and a small quantity of amorphous ice with/or covering crystalline ice could lead to erroneous temperatures. We report in Fig. 4 the reflectance of amorphous and crystalline water ice and the reflectance of the mixture of both (75% of crystalline and 25% of amorphous) at 20 and 80 K. Small shifts appear between pure crystalline water ice and the mixture of amorphous and crystalline water ice, especially for the warmer crystalline ice (wavelength shift of 0.0009 $\mu$m at 80 K compared to 0.0001 $\mu$m at 20 K). The amorphization rate of crystalline water ice by irradiation decreases with increasing temperatures (Strazzulla et al. 1991; Moore & Hudson 1992), and the temperature determination could be biased for a very low-temperature surface covered by a large quantity of amorphous water ice or exposed to irradiation (energetic particles, solar wind, etc.). Nonetheless, this method allows an upper limit on temperature because both effects shift the central wavelengths of the 1.65 $\mu$m toward shorter wavelength (temperatures are higher than foreseen). Moreover, from the high albedo and blue color of 2003 $EL_{61}$ and our surface composition analyses, we can assume a relatively fresh mantle with small amounts of amorphous water ice, allowing us a good confidence level on the results obtained with this spectral thermometer.

Our near infrared spectra have a spectral resolution of 1500, which could allow us to determine the center-band position with high accuracy (0.0007 $\mu$m of accuracy). The signal-to-noise level of our spectra near the 1.65 $\mu$m band is too low to allow direct measurement of the central wavelength of this absorption band. Therefore, we used polynomial curves to fit this absorption feature in the aim of determining its central wavelength. We use several *n*-degrees polynomes (for *n* between 3 and 7 to get a good confidence level), which entirely fits the 1.65 $\mu$m absorption band from 1.63 to 1.69 $\mu$m. From all the fits, we find the minimum close to 1.6567 ± 0.0012 $\mu$m, which corresponds to a surface temperature between 20 and 40 K. This estimation that comes directly from the spectrum gives the mean integrated temperature of this icy surface and does not take the particulate surface properties into account (more or less darker parts of the body, cooler polar zones, etc.). This is compatible with the Stefan-Boltzmann law, even if a better signal-to-noise level is required to increase the accuracy of this measurement.

## 5. Conclusions

Observations of the TNO 2003 $EL_{61}$ carried out with SINFONI and EMMI confirm the presence of large amounts of crystalline water ice on the surface of this body. No clear changes were found between the spectra at different dates (corresponding to different parts of this body), indicating that this object is probably homogeneous despite its elongated shape. Components and constraints used in our radiative transfer models show that amorphous water ice can be a good candidate to fit the bluish spectrum of this object in the near infrared. This observation suggests that the two water ice states are present on the surface of this object, implying crystallization processes (e.g., cryovolcanism) and possibly water ice amorphisation by irradiation (e.g., energetic particles, solar wind). Finally, the good accuracy of our data indicates the surface temperature of the crystalline water ice. Indeed, using the central wavelength of the 1.65 $\mu$m absorption band of the crystalline water ice, we deduce a possible temperature of 20 K with an upper limit around 40 K.

*Acknowledgements.* We thank S. Fornasier and W. Grundy for their help and useful discussions, and we thank J. Emery for useful comments.

## References

Barkume, K. M., Brown, M. E., & Shaller, E. L. 2006, ApJ, 640, L87
Barucci, M. A., Merlin, F., Dotto, E., et al. 2006, A&A, 455, 725
Brown, M. E., Bouchez, A. H., Rabinowitz, D. L., et al. 2005, ApJ, 632, L45
Brown, M. E., Van Dam, A. H., Bouchez, A. H., et al. 2006, ApJ, 639, L46
Brown, M. E., Barkume, K. M., & Shaller, E. L. 2007, Nature, in press
Dumas, C., Hainaut, O. R., Merlin, F., et al. 2007, A&A, submitted
Grundy, W. M., & Schmitt, B. 1998, J. Geophys. Res., 103, 25809
Grundy, W. M., Buie, M. W., Stansberry, J. A., Spencer, J. R., & Schmitt, B. 1999, Icarus, 142, 536
Grundy, W. M., Young, L. A., Spencer, J. R., et al. 2006, Icarus, 184, 543
Hansen, G. B., & McCord, T. B. 2004, J. Geophys. Res. (Planets), 109, 1012
Hapke, B. 1981, JGR, 86 B4, 3039
Hapke, B. 1993, Topics in Remote Sensing (Cambridge, UK: Cambridge University Press)
Hartmann, W., Cruikshank, D. P., & Degewij, J. 1982, Icarus, 52, 377
Jewitt, D. C., & Luu, J. 2004, Nature, 432, 731
Mastrapa, R. M. E., & Brown, R. H. 2002, BAAS, 34, 881
Mastrapa, R. M. E., & Brown, R. H. 2006, Icarus, 183, 207
Moore, M. H., & Hudson, R. L. 1992, ApJ, 401, 353
Rabinowitz, D. L., Barkume, K., Brown, M. E., et al. 2006, ApJ, 639, 1238
Schmitt, B., Quirico, E., Trotta, F., & Grundy, W. M. 1998. Solar System Ices, 199 (Kluwer Academic Publisher)
Strazzulla, G., Leto, G., Baratta, G. A., & Spinella, F. 1991, J. Geophys. Res., 96, 17547
Tegler, S. C., Grundy, W., Consolmagno, G., Romanishin, W., & Mogren, K. 2006, BAAS, 38, 40.01
Trujillo, C. A., Brown, M. E., Barkume, K. A., et al. 2007, ApJ, 655, 1172
Zubko, V. G., Mennella, V., Colangeli, L., & Bussoletti, E. 1996, MNRAS, 282, 1321